Application of anaerobic granular sludge for competitive biosorption of methylene blue and Pb(II): Fluorescence and response surface methodology

Li Shi [a], Dong Wei [b], Huu Hao Ngo [c], Wenshan Guo [c], Bin Du [b], Qin Wei [a] *

[a] *Key Laboratory of Chemical Sensing and Analysis in Universities of Shandong, School of Chemistry and Chemical Engineering, University of Jinan, Jinan 250022, PR China*

[b] *School of Resources and Environment, University of Jinan, Jinan 250022, PR China*

[c] *School of Civil and Environmental Engineering, University of Technology Sydney, Broadway, NSW 2007, Australia*

ABSTRACT

This study assessed the biosorption of anaerobic granular sludge (AGS) and its capacity as a biosorbent to remove Pb(II) and Methylene Blue (MB) from multi-components aqueous solution. It emerged that the biosorption data fitted well to the pseudo-second-order and Langmuir adsorption isotherm models in both single and binary systems. In competitive biosorption systems, Pb(II) and MB will suppress each other's biosorption capacity. Spectroscopic analysis, including Fourier transform infrared spectroscopy (FTIR) and fluorescence spectroscopy were integrated to explain this interaction. Hydroxyl and amine groups in AGS were the key functional groups for sorption. Three-dimensional excitation-emission matrix (3D-EEM) implied that two main protein-like substances were identified and quenched when Pb(II) or

* Corresponding author: Tel: +86 531 82767872; fax: +86 531 82765969
E-mail address: sdjndxwq@163.com (Q. Wei)

MB were present. Response surface methodology (RSM) confirmed that the removal efficiency of Pb(II) and MB reached its peak when the concentration ratios of Pb(II) and MB achieved a constant value of 1.

Keywords: Competitive biosorption; Anaerobic granular sludge; Pb(II); Methylene Blue; Fluorescence spectroscopy; Response surface methodology

1. Introduction

Large quantities of heavy metals and dyes, as typical inorganic and organic toxic compounds, are simultaneous present in wastewater originating from various industries (Körbahti et al., 2011). This hazard wastewater could cause serious damage to ecosystem due to their toxicological properties which pose a major threat to aquatic life forms (Fu and Wang, 2011). It is clearly that not only one single component but also multi-component situations exist in practical wastewater (Wang and Ariyanto, 2007). Therefore, diverse approaches have been employed including biosorption (Yagub et al., 2014), membrane filtration (Wu et al., 1998), and electro-chemical strategies (Shen et al., 2001). Nevertheless, the treatment of these multi-component practical wastewater scenarios (i.e. heavy metals-dyes) is complex and requires effective purification processes (Tovar-Gomez et al., 2013). In particular, of all these above mentioned methods, biosorption is recognized as one of simplest and most cost-effective techniques for treating a variety of pollutants.

Recently, various materials of biological origin were discovered and developed as biosorbents to remove heavy metals and dyes, including biomass, bacteria, activated sludge, and other agricultural by-products, etc. (O'Mahony et al., 2002; Hu,

1996; Comte et al., 2006; Nguyen et al., 2013). Compared to conventional activated sludge, anaerobic granular sludge (AGS) has the advantages of less energy consumption, higher loading, richer biomass, and more abundant functional groups and less residual sludge. Because of its unique granule attributes and abundant binding sites in extracellular polymeric substances (EPS), anaerobic granular sludge is more practical than other biosorbents for treating wastewaters. Several literatures have been reported the adsorption of dyes and heavy metals in mono-component systems (aqueous solutions containing a single dye or metal) by AGS. Liu et al. (2010) demonstrated that three functional groups were identified to play major roles in the adsorption of methylene blue (MB) onto AGS. Van Hullebusch et al. (2005) investigated the sorption capacity and fractionation of sorbed nickel and cobalt onto AGS, suggesting that the key process in controlling the distribution of heavy metals onto AGS was affected by interactions of trace metals-iron sulfide. However, we still do not fully understand the biosorption process for the simultaneous removal of dyes and heavy metals in multi-components systems when AGS as biosorbent is used.

Since the traditional one-factor-at-a-time experiments cannot successfully predict possible interactions between the multi-component industrial effluents (Cao et al., 2010). Therefore, it is vital to develop an efficient method for exploring and elucidating the mechanism in multi-component simultaneous sorption process. Fluorescence spectroscopy which is rapid and has good selectivity and high sensitivity, has been widely employed to characterize EPS. It is generally accepted that EPS from AGS contains abundant fluorescent substances, including proteins and humic

substances which contain large quantities of aromatic structures and unsaturated fatty chains (Li and Yu, 2014). Thus, the structure and key composition of EPS may change after binding with multi-component by using fluorescence spectroscopy. However, until now, little information is available at this point.

Response surface methodology (RSM) is a hybrid of mathematical and statistical methods useful for designing experiments. Lu et al. (2008) used RSM to explore and predict competitive biosorption when different metal compositions interact, demonstrating that the parameters of the empirical model can estimate the multi-metal biosorption process more effectively when employing RSM. For the above reasons, RSM was selected to explain the interactions of multi-components.

Based on the above discussion, the objective of this study was to evaluate the biosorption and interaction mechanism of simultaneous removal of multi-component systems from wastewater onto AGS using fluorescence spectroscopy and optimization via RSM. Pb(II) and MB were selected as the typical heavy metal ion and dye, respectively. Single and binary systems were compared to investigate the simultaneous adsorption process and determine the biosorption kinetics and isotherm. A combined use of three-dimensional excitation-emission matrix (3D-EEM) fluorescence spectroscopy and synchronous fluorescence spectra were served to explain the mechanism of the interaction between EPS and contaminant. Box-Behnken design (BBD) helped to explore the behavior of multi-component biosorption.

2. Materials and methods

2.1. Reagents and materials

All chemicals, MB ($C_{16}H_{18}N_3SCl$, MW 373.90) and Lead (II) nitrate [$Pb(NO_3)_2$, 99.0%], were obtained from Sinopharm Chemical Reagent Beijing Co. Ltd., China and of analytical reagent grade without further purification. Ultrapure water (EASY-pure LF, Barnstead International, Dubuque, IA, USA) was used throughout the experiment.

Anaerobic granular sludge was taken from an up-flow anaerobic sludge bed (UASB) reactor treating soy protein wastewater, located in Shandong province in China (treatment capacity 2500 m^3/day). The average size of anaerobic granular sludge used in this study was about 2 mm. Before biosorption experiments, anaerobic granular sludge was gently washed three times by using deionized water to remove the surface soluble ions. Then it was dried in an oven at 60 °C for 24 h. The resulting dried sludge was stored in a desiccator for further use.

2.2. Preparation of Lead and MB stock solution

A stock solution of Pb(II), was obtained by dissolving the exact quantity of $Pb(NO_3)_2$ in Milli-Q water. The dye stock solutions were prepared by dissolving accurately weighed dyes in deionized water to the concentration of 1000 mg/L and subsequently diluted when necessary. The ranges of concentrations of both metal ions and dye ions prepared from stock solutions varied between 50 mg/L and 500 mg/L.

For the investigation with binary metal-dye solutions, the desired combinations of Pb(II)-MB ions were obtained by diluting 1000 mg/L of stock solutions of metal

ions and dye ions and mixing them in the test medium. In this case, the mass ratios of initial concentrations of Pb(II)-MB were 1:1 over a metal-dye concentration range of 50 to 500 mg/L. Before mixing with the biosorbent, the pH of each test solution was adjusted to 6 with 0.1 mol/L HNO_3 and NaOH.

2.3. Batch biosorption experiments

Biosorption kinetic experiments in both single and binary biosorption systems were conducted. For the single biosorption system experiment, around 0.4 g (dry weight) of anaerobic granular sludge was added to 100 mL of Pb(II) or MB solutions of different initial concentrations (50, 100, 150 mg/L for Pb(II) and MB). Then the mixed solution was stirred for 5 to 120 min at 150 rpm at 25°C. For the binary biosorption system experiment, Pb(II) and MB were mixed to create a solution (100mL) containing 100mg/L Pb(II) and 100mg/L MB. Then 0.4 g of AGS were added and stirred for 5 to 120 min at 150 rpm at 25°C. Samples were taken at predetermined time intervals to analyze the of Pb(II) and MB concentrations.

The biosorption isotherm experiment was done with different initial concentrations of Pb(II) and MB from 50 to 500 mg/L. For binary systems, the metal-dye mixed solution concentration ratio was always maintained at 1:1 (v/v) from 50 to 500mg/L and stirred for biosorption equilibrium.

The amount of adsorbed metal and dye q_t (mg/g) at different time t, was calculated using the following Eq. (1):

$$q_t = \frac{(C_0 - C_t) \times V}{W} \quad (1)$$

Where C_0 (mg/L) and C_t (mg/L) are the initial concentration of metal or dye and

the concentration at time t, respectively. V (L) stands for the volume of solution, and W (g) is the mass of adsorbent.

2.4. EPS extraction and 3D-EEM

Heating method was wildly used to extract EPS from sludge because it was convenient with a relatively high extraction yield and low cellular lysis (Li and Yang, 2007). Therefore, a modified heat extraction method was selected to extract EPS from anaerobic granular sludge according to previous literature reported by Xu et al. (2010). Briefly, 25 mL anaerobic granular sludge was first washed three times with deionized water, and then centrifuged in a 50 mL tube at 4000 rpm for 5 min to remove the supernatant. After that, the cell pellet was re-suspended with 0.05% NaCl solution and heated at 80°C for 1 h, and then centrifuged at 10000 rpm for 15 min. Finally, the supernatant was filtered through a 0.45 μm pore size filter. The collected filtrate was considered to be the EPS of anaerobic granules sludge.

All 3D-EEM fluorescence spectra of the EPS solution were recorded with a fluorescence spectrophotometer (LS-55, Perkin-Elmer Co., USA). The EEM spectra were collected at 10 nm increments over an excitation range of 200-400 nm, with an emission range of 280-550 nm by every 0.5 nm. The excitation and emission slits were set to 10 nm and 10 nm of band-pass, respectively.

2.5. Fluorescence quenching titration

To investigate the mechanism of fluorescence quenching between EPS, Pb(II), and MB, quenching titration tests of synchronous fluorescence spectra of EPS before and after binding with different Pb(II) or MB concentrations were conducted. More

detailed, 2 mL extracted EPS solution was added into a 10 mL centrifugal tube, and 2 mL different concentrations of pre-determined Pb(II) or MB solution and 6 mL deionized water were successively added to ensure the final Pb(II) or MB concentrations varied from 0 to 30 mg/L. The pH value was adjusted to 6.0 and the temperature was set at 25°C. Then the solutions were mixed for 2 h using an oscillator prior to spectral analysis.

Synchronous fluorescence spectra were recorded by scanning excitation wavelengths ranging from 230 to 350 nm with a constant offset ($\Delta\lambda$ at 60 nm). Both excitation and emission slits were adjusted to 10 nm and the scan speed was set at 1200 nm/min.

2.6. Response surface methodology (RSM)

RSM has been generally applied to create the best experimental conditions. However, this method was rarely used to: firstly, interpret the interaction of co-existing metal-dye during the biosorption process; and secondly, predict multi-component biosorption results. Box–Behnken design (BBD) explored the behavior of multi-component biosorption onto AGS. In this study, 17 runs for a three-parameter experimental design were required by BBD. A mathematical relationship between the three independent factors can be approximated by the second order polynomial model according to Eq. (2) as follows:

$$Y = \beta_0 + \sum_{i=1}^{3} \beta_i X_i + \sum_{i=1}^{3} \sum_{j=1}^{3} \beta_{ij} X_i X_j + \sum_{i=1}^{3} \beta_{ii} X_i^2 + \varepsilon \quad (2)$$

Where Y is the predicted response, β_0 is the coefficient of intercept, β_i is the

coefficient of linear effect, β_{ii} is the coefficient of quadratic effect, β_{ij} is the coefficient of interaction effect, ε is a random error, and X_i and X_j are coded predicted variables for the independent factors. The software used for experimental design and doing the data analysis was Design-Expert 8.0.6.

2.7. Analytical methods

The concentrations of heavy metal ions in solution were determined by Atomic Adsorption Spectroscopy (AAS) (AA-7000, Shimadzu, Japan). The analysis of MB in the filtered solutions was done using an UV/vis spectroscopy (TU-1901, Purkinje General Instrument Co. Ltd. China) at 665 nm. The Fourier transform infrared spectroscopy (FTIR) of EPS was recorded on VERTEX70 FTIR spectrometer (Bruker Co., Germany). All the samples were monitored immediately in this study. The experiments were conducted in triplicate and the negative controls (with no sorbent) were simultaneously carried out to ensure that sorption was caused only by AGS. The experimental error of results was within ± 5%.

3. Results and discussion

3.1. Biosorption kinetics

Kinetic biosorption of MB or Pb(II) was investigated in the single biosorption system first. The effect of initial concentration of MB and Pb(II) on the sorption capacity of the AGS at various contact times is presented in Fig. 1A and 1B.

For a smaller concentration of MB (50 mg/L), most adsorption took place in the first 25 min. After this, the rates of biosorption were negligible and residual MB

194 concentration in solution reached an almost constant value. However, at the initial dye
195 concentrations of 100 and 150 mg/L of MB, they both took 45 min to reach
196 equilibrium. However, Pb(II) solution with different initial concentrations (50, 100
197 and 150 mg/L) took the same time to reach equilibrium at about 60 min.

198 In order to predict the kinetics of the present sorption process, firstly, the
199 pseudo-first-order kinetic model was defined as Eq. (3), and secondly, the
200 pseudo-second-order kinetic model was expressed as the following Eq. (4):

201 $$\log\left(q_e - q_t\right) = \log q_e - \frac{k_1}{2.303} t \quad (3)$$

202 $$\frac{t}{q_t} = \frac{1}{k_2 q_e^{\,2}} + \frac{t}{q_e} \quad (4)$$

203 Where q_e and q_t (mg/g) are the amount of MB adsorbed onto per gram of
204 adsorbent at equilibrium and at time t (min), respectively, and k_1 (min^{-1}) is the
205 pseudo-first-order rate constant. k_2 (g/mg·min) is the pseudo-second-order rate
206 constant. Modeling of kinetics models and parameters obtained from the pseudo-first-
207 and second-order models are documented in Table 1. It was found that the
208 pseudo-second-order model has a higher correlation coefficient R^2. Biosorption
209 capacities calculated by the pseudo-second-order were also close to those obtained in
210 the experiments.

211 In order to investigate the competitive biosorption kinetics, MB and Pb(II)
212 adsorption onto AGS in the binary system as a function of contact time was studied
213 (Fig. 1C). The high R^2 (0.99 for MB and 0.99 for Pb(II) in Table 1) revealed that the
214 competitive biosorption of MB and Pb(II) followed the pseudo-second order model
215 well. The presence of MB had no significant impact on the equilibrium time of Pb(II)

adsorption. However, the adsorbed amount of Pb(II) declined from 39.77 mg/g to 37.52 mg/g. Equilibrium time of MB adsorption increased from 45 min to 90 min due to the presence of Pb(II), but the adsorbed amount fell slightly from 37.10 mg/g to 34.94 mg/g. Therefore, the presence of MB reduced the amount of Pb(II) adsorption slightly, while the presence of Pb(II) also decreased the rate of MB adsorption.

3.2. Biosorption isotherms

The most popular biosorption model is the Langmuir model (Langmuir, 1916). It is not only used to predict of single adsorption but for multi-adsorption as well. It is most commonly used for monolayer adsorption on to a surface with a finite number of identical sites, as shown by Eq. (5) as follows:

$$q_e = \frac{q_m K_L C_e}{1 + K_L C_e} \tag{5}$$

Where C_e is the equilibrium concentration of MB (mg/L); q_e is the amount of MB adsorbed (mg/g); q_m is the theoretical maximum monolayer sorption capacity (mg/g); and K_L is the Langmuir adsorption equilibrium constant (L/mg) related to the affinity of the sorbent for the solute.

The presence of one metal species reduced the sorption capacity of the other (Papageorgiou et al., 2009). To analyze the nature of competition between MB and Pb(II), the Langmuir competitive model (Hossain et al., 2014), was applied to the binary sorption equilibrium data as indicated in Eq. (6):

$$q_{e.i} = \frac{q_{m.i} K_{L.i} (C_{e.i})}{1 + \sum_{j=1}^{N} K_{L.j} (C_{e.j})} \tag{6}$$

Where, $q_{e.i}$ is the equilibrium adsorption capacity (mg/g) for i mixture of the

237 solutes at equilibrium concentration, $C_{e.i}$ (mg/L), $K_{L.i}$; Langmuir isotherm parameter
238 for mixture *i* of the solutes and $q_{m.i}$, maximum adsorption capacity for *i* mixture of the
239 solutes (mg/g). *j*= number of component in the solution. The parameters obtained
240 from the single and binary systems isotherm models are depicted in Table 2. The
241 Langmuir equation fitted well to both the mono- and multi- experimental results.
242 Based on the Langmuir isotherm, the maximum adsorption capacities of MB and
243 Pb(II) obtained from binary systems sorption were less than those obtained from the
244 single system (Table 2).

245 ***3.3. Biosorption selectivity in binary system***

246 Relative biosorption of MB and Pb(II) in the binary system was calculated using
247 the following equation Eq. (7) (Wang and Ariyanto, 2007):

248 $$A_r = \frac{[q_t]_B}{[q_t]_S} \quad (7)$$

249 Where $[q_t]_B$ and $[q_t]_S$ are the amount of biosorption of a specific adsorbate in the
250 binary system and the single system at time t, respectively. Biosorption selectivity in
251 the binary system was defined as Eq. (8):

252 $$S = \frac{(A_r)_{Pb}}{(A_r)_{MB}} \quad (8)$$

253 Fig. S1 shows the variation of relative biosorption of MB and Pb(II) and the
254 biosorption selectivity in the binary system with time. As can be seen from Fig. S1,
255 the relative biosorption of MB was low in the initial 60 min, indicating biosorption of
256 MB in the binary system was inhibited by the presence of Pb(II). Meanwhile, relative
257 biosorption of Pb(II) exhibited a slightly higher ratio than MB. This could mean that

Pb(II) dominanted during the at initial stages.

Biosorption revealed a tendency to decrease and approached a constant value of 1. The difference between relative biosorption of MB and Pb(II) suggests that AGS has a higher affinity to Pb(II) biosorption in the binary system. Biosorption's decrease confirms that the biosorption favors Pb(II). When the biosorption approaches equilibrium, biosorption will be the same for MB and Pb(II).

In the single system, AGS has many functional groups with a negative charge. This enables Pb(II) and MB to both show a positive electrostatic charge will contact AGS more easily and be adsorbed sequentially (Yao et al., 2010). Nevertheless, in the binary system the Pb(II) will have produced an electrostatic repulsion with the MB. Consequently this could explain why the removal efficiency of MB will decrease when Pb(II) is present.

3.4. FTIR spectroscopy

The FTIR spectra of raw, metal-loaded, dye-loaded and metal-dye-loaded granules in the 400–4000 cm^{-1} range were taken to obtain information on the nature of possible interactions between the functional groups of AGS, the metal ions and dye (see Fig. S2). The infrared spectrum of fresh AGS exhibits broad bands centered at 3283 cm^{-1} assigned to O–H and N–H stretching, C–H stretching vibrations at 2925 cm^{-1}, the stretching vibration of C–O and C–N (amide I) peptidic bond of protein at 1655 cm^{-1}, stretching vibration of C–N and deformation vibration of N–H (amide II) peptidic bond of protein at 1542 cm^{-1},C–H bending vibration at 1385 cm^{-1}, C–O stretching of alcoholic groups at 1061 cm^{-1} (Park et al., 2005).

Fig. S2 spectra b–d highlight the changes in the granules' spectrum following the sorption of Pb(II) and MB. After exposure to MB and Pb(II), the broad overlapping region for N–H and O–H stretching in the 3200–3500 cm^{-1} range also presented some changes, but it was difficult to distinguish which group causes the shift. The peak at 1640–1660 cm^{-1} which corresponded to the superimposition of different amide I band (C–O stretching coupled with N–H deformation mode) from different materials (including proteins, amide-bearing materials), was significantly decreased. This indicated the complexion of metal and dye ions with the functional groups from protein. It may also indicate the significant role of amine groups in the biosorption process.

Compared to the intensities of the C–O stretching of the hydroxyl group (C–O–H) from saccharides at 1061 cm^{-1}, the peak shifted to the following lower wave numbers 1053, 1047 and 1045 cm^{-1} for MB, Pb(II) and Pb(II)-MB-loaded granules respectively, thus demonstrating that hydroxyl groups were involved in the metal and dye biosorption. Finally, it should be noted that intensity decreases with band shifts of the peaks in the region of lower wavenumbers (under 700 cm^{-1}) after metal sorption, This could be attributed to an interaction between both metal ions and N-containing ligands (Alt & Wagner, 2009). These changes observed in the spectrum indicated the possible involvement of functional groups on the surface of the AGS in the biosorption process.

3.5. Fluorescence spectra

3.5.1 3D-EEM fluorescence spectra

3D-EEM can present detailed information about the chemical composition of EPS samples as a spectral fingerprint technology (Wei et al., 2015). It has been extensively used for characterizing dissolved organic matter (DOM) in water and wastewater treatment (Wu and Tanoue, 2001; Baker, 2002). Fig. 2 shows 3D-EEM fluorescence spectra of EPS with Pb(II), MB and Pb(II)-MB. The fluorescence spectra parameters of EPS samples, including peak location and fluorescence intensity, are summarized in Table 3.

In Fig. 2A it can be seen that two fluorescence peaks (Peak A and B) were obviously identified in the control EPS without the presence of Pb(II) or MB. Peaks A and B could be assigned to protein-like fluorescence (Yamashita & Tanoue, 2003; Baker & Inverarity, 2004). Peak A and Peak B were identified at Ex/Em of 230 nm/350-365 nm and 280/350-356 nm, respectively. The fluorescence intensities were very different in the presence of Pb(II) or MB. The Pb(II) would made Peak A drop significantly from 974.16 to 770, but the decreased in Peak B was very slight, only from 753.83 to 710.21. Compared to the presence of single Pb(II), a mono-MB system would made Peak B's decrease more significant to approximately 371.37. Peak A betrayed a small decrease only to 75.09. In the presence of Pb(II)-MB, the fluorescence intensities of these two major types of substances gradually decreased from 974.16 and 753.83 to 691.73 and 359.95 (Table 3), respectively. This outcome suggests that the two main components of EPS were obviously quenched when Pb(II) and MB were added. The results further confirmed that EPS plays a definite role in the migration and removal of Pb(II) and MB in the biosorption process.

3.5.2 Synchronous fluorescence

The synchronous fluorescence spectra intensities also decreased markedly with increasing Pb(II) and MB concentration (Fig. 3). The data of fluorescence intensities systematically declined from 852.83 to 645.26 and 98.54 when Pb(II) and MB concentrations increased. This outcome revealed that the main contribution to fluorescence quenching of EPS was caused by a PN-like substance, which is consistent with the previous result of 3D-EEM (Fig. 2).

Dynamic and static quenching are generally the two major mechanisms of fluorescence quenching, depending on the method of interaction (collision or complexation) between quencher and fluorophore. The fluorescence quenching data can be modeled using the Stern-Volmer equation (Eq. (9)):

$$\frac{F_0}{F} = 1 + K[Q] = 1 + k_q \tau_0 [Q] \quad (9)$$

Where F_0 and F of the fluorophore are the fluorescence intensities in the absence and presence of Pb(II) or MB, respectively. K is the Stern-Volmer quenching rate constant. [Q] is the Pb(II) or MB concentration. k_q is the quenching rate constant of the biological macromolecule, and τ_0 is the average lifetime of the molecule.

Normally, the Stern-Volmer plot is linear if the quenching type is generally indicative of a single static or dynamic quenching, while the Stern-Volmer plot exhibits an upward curvature at high [Q] if the quenching type is a combined quenching (Gong et al., 2007). The Stern-Volmer plot is linear at high [Pb(II)] (Fig. 4A) which means that dynamic quenching or static quenching barely occurred between EPS and Pb(II). However, exhibiting an upward curvature with high [MB]

(Fig. 4A), indicates that dynamic quenching and static fluorescence quenching occurred simultaneously between EPS and MB in this study. In addition, the much larger values of kq (Table 4) than 2.0×10^{10} $L\cdot mol^{-1}\cdot S^{-1}$ also indicated the static quenching process (Hu et al., 2005).

To better understand the static quenching mechanism an analysis was conducted of the fluorescence quenching data using the Stern-Volmer equation (Eq. (10)):

$$\frac{1}{(F_0 - F)} = \frac{1}{F_0 K_a [MB]} + \frac{1}{F_0} \quad (10)$$

Where K_a is the effective quenching constant. K_a was calculated as 7.97×10^4 L/mol and 4.94×10^4 L/mol for Pb(II) and MB. The high binding constants (K_a, 10^4-$10^5 M^{-1}$) (Table 4) and the data from quenching experiments confirm that static quenching was the predominant form of quenching throughout the EPS-Pb(II) and EPS-MB complex system (Fig. 4B). Consequently, Pb(II) and MB can be migrated and removed by EPS during wastewater treatment.

3.5. RSM and model fit

In order to determine the competitive biosorption operating parameters, contact time, different initial concentrations of Pb(II) and different initial concentrations of MB were investigated individually for their effect on competitive biosorption by AGS. The actual values of process variables and their variation limits were selected based on the values obtained in preliminary experiments and coded as shown in Table S1. The $[(A_r)_{Pb}+(A_r)_{MB}]$ (Y (%)) instead of removal efficiency was considered to be the dependent factor (response).

Subsequently, a quadratic polynomial equation could be determined by BBD to

368 evaluate the competitive biosorption capacity by AGS, which was given as follows in
369 Eq. (11):

370 $$Y = 1.89 + 0.35A + 0.36B + 0.065C - 0.13AB + 0.03AC + 0.044BC - 0.51A^2 - 0.50B^2 - 0.028C^2 \quad (11)$$

371 To investigate the predictability of the RSM model and the significance of the
372 influences, Analysis of Variance (ANOVA) test was conducted and the results are
373 provided in Table S2. It can be seen from Table S2 that Prob > F less than 0.05
374 indicated model terms were significant. Similarly, the P-values for A, B, AB, A^2 and
375 B^2 were all less than 0.0001, indicating that they were all significant for competitive
376 biosorption by AGS.

377 Additionally, the quadratic model showed correlation coefficient (R^2) of 0.9982
378 between actual and predicted values. This means the model explains 99.82% of
379 variation around the average. Furthermore, the coefficient of variation (C.V.) of 2.21%
380 demonstrated a satisfying precision and reliability of the established model. Therefore,
381 the BBD model could reasonably estimate the response of the competitive biosorption
382 by AGS.

383 To visualize the relationship between the response and the level of each
384 operating factor, a three-dimensional plot was established to investigate the influences
385 of these three factors on competitive biosorption by AGS. According to the ANOVA
386 results in Table S2, the different initial concentrations of Pb(II) and different initial
387 concentrations of MB were found to be more significant than contact time. This was
388 because the selected time is equilibrium time which has little effect on the removal of
389 both Pb(II) and MB. Therefore, the three-dimensional plot of the combined different

initial concentrations of Pb(II) and different initial concentrations of MB at a optimal contact time are given in Fig. 5. As observed in Fig. 5, the $[(A_r)_{Pb}+(A_r)_{MB}]$ increased with different initial concentrations of Pb(II) and different initial concentrations of MB.

During the initial stage, sorption sites did not reach saturation so the $[(A_r)_{Pb}+(A_r)_{MB}]$ values increased when the concentrations also increased. However, with rising Pb(II) and MB's concentrations, the sorption sites will achieve saturation and the $[(A_r)_{Pb}+(A_r)_{MB}]$ values would be at their maximum. At the final stage, Pb(II) and MB would be comprtitive but the sorption sites will have the same affinity for both. This will decrease the $[(A_r)_{Pb}+(A_r)_{MB}]$ values. Based on the 3D surface plots, the optimized conditions for the competitive biosorption by AGS were determined to be 338.38 mg/L Pb(II), 340.65 mg/L MB and contact time of 122.61 min with a maximum value 1.89 of $[(A_r)_{Pb}+(A_r)_{MB}]$. The concentrations ratios of Pb(II) and MB approach a constant value of 1 and this means the results were consistent with biosorption selectivity.

4. Conclusions

This study proved that AGS could be used as an effective and practical biosorbent for treating wastewater containing multi-components. Results showed that the biosorption data fitted well to the pseudo-second-order model and Langmuir adsorption isotherm model in both single and binary systems. The fluorescence spectroscopy effectively evaluated the sorption and interaction mechanism of EPS-Pb(II) and EPS-MB. Furthermore the RSM proved to be ideal for experimental

conditions involving multi-component biosorption. Subsequently, the results of this study provide useful information that AGS has potential broad application for the treatment of wastewater containing metal-dye effluent.

Acknowledgments

This study was supported by the Natural Science Foundation of Chinese Province (21377046), Special project of independent innovation and achievements transformation of Shandong Province (2014ZZCX05101), Science and technology development plan project of Shandong province (2014GGH217006), and QW thanks the Special Foundation for Taishan Scholar Professorship of Shandong Province and UJN (No.ts20130937).

References

[1] Alt, H. C., & Wagner, H. E. (2009). Comparative mid-and far-infrared spectroscopy of nitrogen–oxygen complexes in silicon. Physica B: Condensed Matter, 404, 4549-4551.

[2] Baker, A. (2002). Fluorescence properties of some farm wastes: implications for water quality monitoring. Water Research, 36, 189-195.

[3] Baker, A., & Inverarity, R. (2004). Protein‐like fluorescence intensity as a possible tool for determining river water quality. Hydrological Processes, 18, 2927-2945.

[4] Cao, Y. R., Liu, Z., Cheng, G. L., Jing, X. B., & Xu, H. (2010). Exploring single and multi-metal biosorption by immobilized spent Tricholoma lobayense using multi-step response surface methodology. Chemical Engineering Journal, 164(1),

183-195.

[5] Comte, S., Guibaud, G., & Baudu, M. (2006). Biosorption properties of extracellular polymeric substances (EPS) resulting from activated sludge according to their type: soluble or bound. Process Biochemistry, 41(4), 815-823.

[6] Fu, F., & Wang, Q. (2011). Removal of heavy metal ions from wastewaters: a review. Journal of Environmental Management, 92(3), 407-418.

[7] Gong, A., Zhu, X., Hu, Y., & Yu, S. (2007). A fluorescence spectroscopic study of the interaction between epristeride and bovin serum albumine and its analytical application. Talanta, 73, 668-673.

[8] Hossain, M. A., Ngo, H. H., Guo, W. S., Nghiem, L. D., Hai, F. I., Vigneswaran, S., & Nguyen, T. V. (2014). Competitive adsorption of metals on cabbage waste from multi-metal solutions. Bioresource Technology, 160, 79-88.

[9] Hu, T. L. (1996). Removal of reactive dyes from aqueous solution by different bacterial genera. Water Science and Technology, 34(10), 89-95.

[10] Hu, Y. J., Liu, Y., Zhang, L. X., Zhao, R. M., & Qu, S. S. (2005). Studies of interaction between colchicine and bovine serum albumin by fluorescence quenching method. Journal of Molecular Structure, 750, 174-178.

[11] Körbahti, B. K., Artut, K., Geçgel, C., & Özer, A. (2011). Electrochemical decolorization of textile dyes and removal of metal ions from textile dye and metal ion binary mixtures. Chemical Engineering Journal, 173(3), 677-688.

[12] Langmuir, I. (1916). The constitution and fundamental properties of solids and liquids. Part 1. Solids. Journal of the American Chemical Society, 38(11),

2221-2295.

[13] Li, W. W., & Yu, H. Q. (2014). Insight into the roles of microbial extracellular polymer substances in metal biosorption. Bioresource Technology, 160, 15-23.

[14] Liu, F., Teng, S., Song, R., & Wang, S. (2010). Adsorption of methylene blue on anaerobic granular sludge: Effect of functional groups. Desalination, 263(1), 11-17.

[15] Lu, W. B., Kao, W. C., Shi, J. J., & Chang, J. S. (2008). Exploring multi-metal biosorption by indigenous metal-hyperresistant Enterobacter sp. J1 using experimental design methodologies. Journal of Hazardous Materials, 153(1), 372-381.

[16] Nguyen, T. A. H., Ngo, H. H., Guo, W. S., Zhang, J., Liang, S., Yue, Q. Y., Li, Q & Nguyen, T. V. (2013). Applicability of agricultural waste and by-products for adsorptive removal of heavy metals from wastewater. Bioresource Technology, 148, 574-585.

[17] O'mahony, T., Guibal, E., & Tobin, J. M. (2002). Reactive dye biosorption by Rhizopus arrhizus biomass. Enzyme and Microbial Technology, 31(4), 456-463.

[18] Papageorgiou, S. K., Katsaros, F. K., Kouvelos, E. P., & Kanellopoulos, N. K. (2009). Prediction of binary adsorption isotherms of Cu^{2+}, Cd^{2+} and Pb^{2+} on calcium alginate beads from single adsorption data. Journal of Hazardous Materials, 162(2), 1347-1354.

[19] Shen, Z., Wang, W., Jia, J., Ye, J., Feng, X., & Peng, A. (2001). Degradation of dye solution by an activated carbon fiber electrode electrolysis system. Journal of

Hazardous Materials, 84(1), 107-116.

[20] Tovar-Gomez, R., Rivera-Ramírez, D. A., Hernandez-Montoya, V., Bonilla-Petriciolet, A., Durán-Valle, C. J., & Montes-Moran, M. A. (2012). Synergic adsorption in the simultaneous removal of acid blue 25 and heavy metals from water using a Ca $(PO_3)_2$-modified carbon. Journal of Hazardous Materials, 199, 290-300.

[21] Van Hullebusch, E. D., Peerbolte, A., Zandvoort, M. H., & Lens, P. N. (2005). Sorption of cobalt and nickel on anaerobic granular sludges: isotherms and sequential extraction. Chemosphere, 58(4), 493-505.

[22] Wang, S., & Ariyanto, E. (2007). Competitive adsorption of malachite green and Pb ions on natural zeolite. Journal of Colloid and Interface Science, 314(1), 25-31.

[23] Wei, D., Shi, L., Yan, T., Zhang, G., Wang, Y., & Du, B. (2014). Aerobic granules formation and simultaneous nitrogen and phosphorus removal treating high strength ammonia wastewater in sequencing batch reactor. Bioresource Technology, 171, 211-216.

[24] Wei, D., Wang, B., Ngo, H. H., Guo, W., Han, F., Wang, X., Du, B. & Wei, Q. (2015). Role of extracellular polymeric substances in biosorption of dye wastewater using aerobic granular sludge. Bioresource Technology, 185, 14-20.

[25] Wu, F., & Tanoue, E. (2001). Isolation and partial characterization of dissolved copper-complexing ligands in streamwaters. Environmental Science & Technology, 35, 3646-3652.

[26] Wu, J., Eiteman, M. A., & Law, S. E. (1998). Evaluation of membrane filtration and ozonation processes for treatment of reactive-dye wastewater. Journal of Environmental Engineering, 124(3), 272-277.

[27] Xu, J., Sheng, G. P., Ma, Y., Wang, L. F., & Yu, H. Q., (2013). Roles of extracellular polymeric substances (EPS) in the migration and removal of sulfamethazine in activated sludge system. Water Research, 47, 5298-5306.

[28] Yagub, M. T., Sen, T. K., Afroze, S., & Ang, H. M. (2014). Dye and its removal from aqueous solution by adsorption: A review. Advances in Colloid and Interface Science, 209, 172-184.

[29] Yao, Y., Xu, F., Chen, M., Xu, Z., & Zhu, Z. (2010). Adsorption behavior of methylene blue on carbon nanotubes. Bioresource Technology, 101(9), 3040-3046.

[30] Yamashita, Y., & Tanoue, E. (2003). Chemical characterization of protein-like fluorophores in DOM in relation to aromatic amino acids. Marine Chemistry, 82, 255-271.

516 **Figure Captions**

517 **Fig.1** Effect of contact time on (A) Single-MB (B) Single-Pb(II) and (C)
518 Binary-MB-Pb(II).

519 **Fig. 2** The exemplified 3D-EEM fluorescence spectra of EPS with Pb(II) and MB: (A)
520 EPS, (B) EPS-MB, (C) EPS-Pb(II) and (D) EPS-MB-Pb(II).

521 **Fig. 3** The synchronous fluorescence spectra for quenching of EPS titrated with MB
522 (A) and Pb(II) (B).

523 **Fig. 4** The Stern-Volmer (A) and Modified Stern-Volmer (B) plots of fluorescence
524 emission for quenching of EPS titrated with MB and Pb(II).

525 **Fig. 5** Response surface plot for the effect on MB concentration, Pb(II) concentration
526 and their mutual effect on the $[(Ar)_{Pb}+(Ar)_{MB}]$.

527

528

529

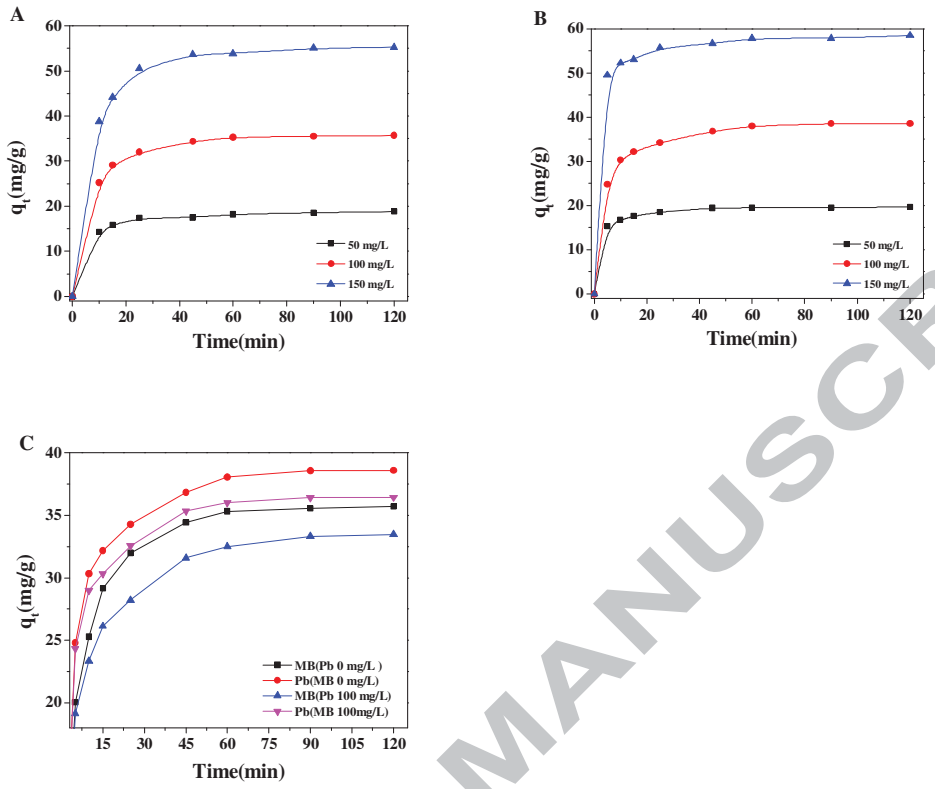

530 **Fig. 1** Effect of contact time on (A) Single-MB (B) Single-Pb(II) and (C)

531 Binary-MB-Pb(II).

532

533

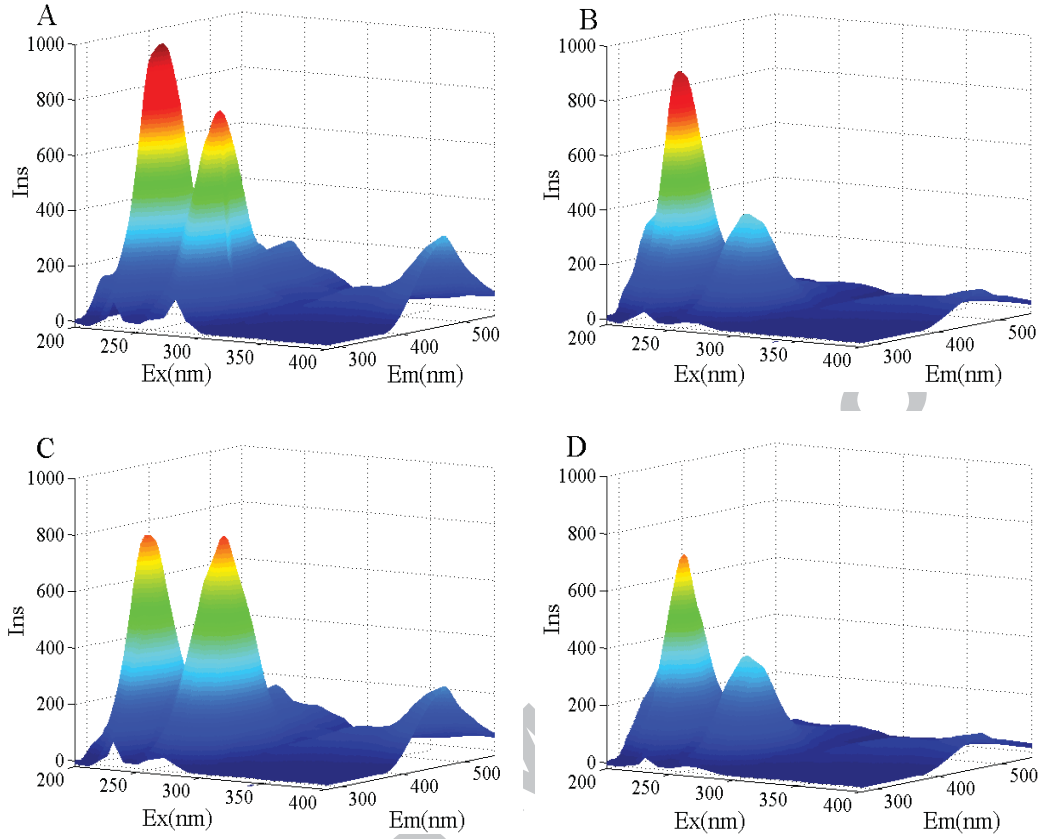

534 **Fig. 2** The exemplified 3D-EEM fluorescence spectra of EPS with Pb(II) and MB: (A)

535 EPS, (B) EPS-MB, (C) EPS-Pb(II) and (D) EPS-MB-Pb(II).

536

537

538

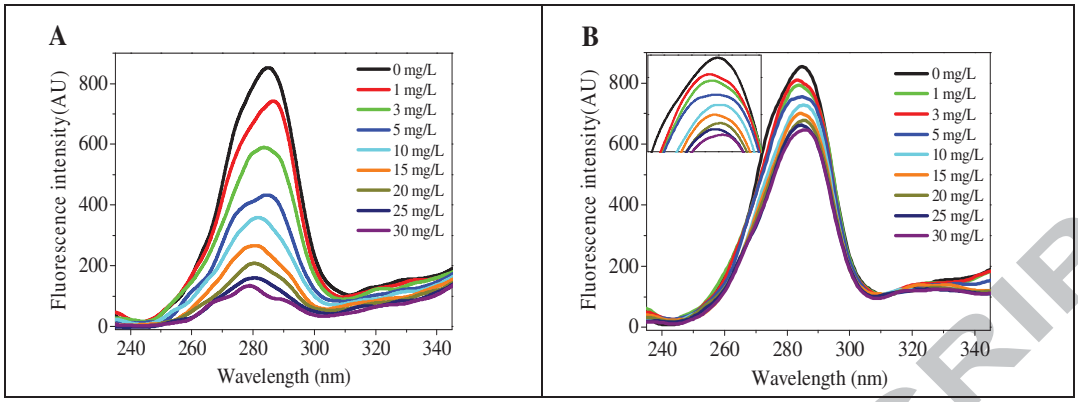

539 **Fig. 3** The synchronous fluorescence spectra for quenching of EPS titrated with MB

540 (A) and Pb(II) (B).

541

542

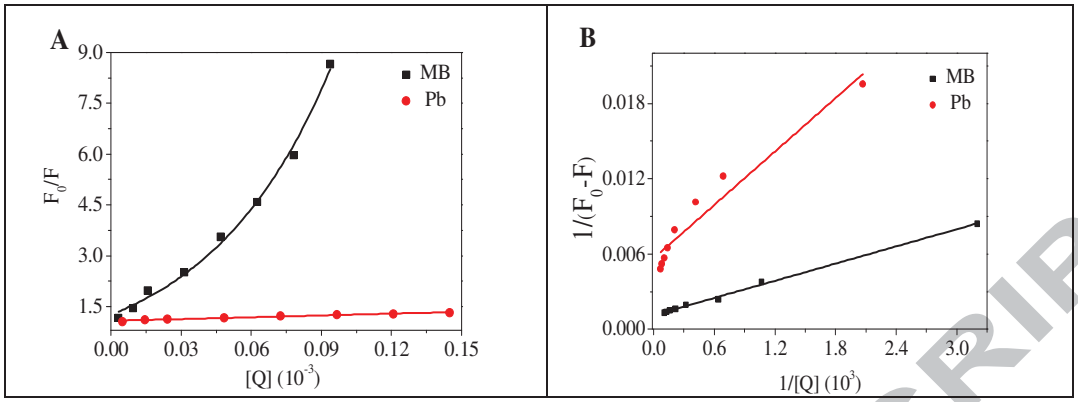

543 **Fig. 4** The Stern-Volmer(A) and Modified Stern-Volmer(B) plots of fluorescence

544 emission for quenching of EPS titrated with MB and Pb(II).

545

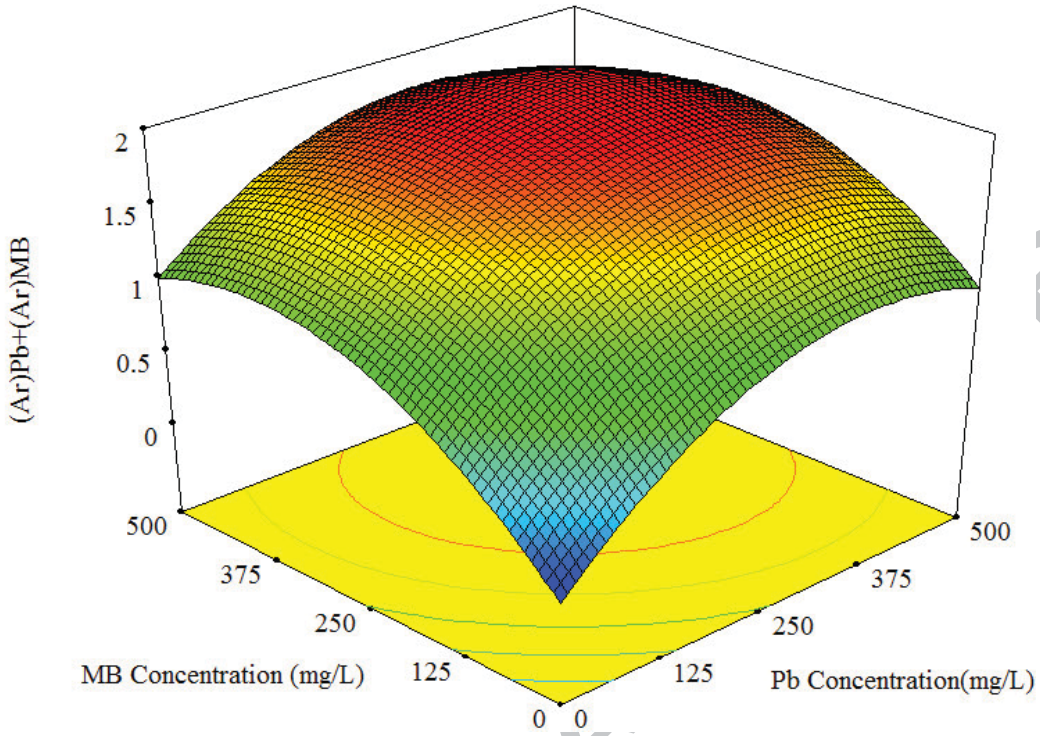

546

547 **Fig. 5** Response surface plot for the effect on MB concentration, Pb(II) concentration

548 and their mutual effect on the $[(Ar)_{Pb}+(Ar)_{MB}]$.

549

550

551

552 **Table 1** Kinetics constants for adsorption in single and binary systems

Adsorbate	C_0(mg/L)	Pseudo first-order			Pseudo second-order	
		k_1 (min^{-1})	q_e (mg/g)	R^2	k_2(g/mg min)	q_e (mg/g)
Single system						
MB	50	0.021	5.23	0.88	0.015	19.29
	100	0.021	11.06	0.79	0.007	37.10
	150	0.020	17.84	0.76	0.003	57.63
Pb(II)	50	0.023	3.06	0.78	0.029	19.97
	100	0.022	10.55	0.86	0.008	39.77
	150	0.021	14.38	0.91	0.005	60.24
Binary system						
MB	100	0.021	12.16	0.88	0.005	34.94
Pb(II)	100	0.022	9.48	0.83	0.008	37.52

553

554 **Table 2** Parameters of Langmuir for biosorption isotherm of MB and Pb(II) on AGS
555 in single and binary system

Adsorbate Equilibrium parameters	q_m.Exp(mg/g)	q_m.Mod(mg/g)	K_L(L/g)	R^2
Single				
MB	86	107.64	0.0365	0.99
Pb(II)	97.49	111.24	0.0809	0.97
Binary				
MB	68.88	75.01	0.0597	0.99
Pb(II)	78.53	83.19	0.0774	0.99

556

557 **Table 3** Effects of Methylene blue and Pb(II) on the peak intensity of EPS.

	Peak A			Peak B		
Sample	Ex	Em	Ins	Ex	Em	Ins
EPS	230	360	974.16	280	351	753.83
EPS+MB	230	356	875.09	280	361	371.37
EPS+Pb	230	352	770.00	280	356	710.21
EPS+MB+Pb	230	363	691.73	280	360	359.95

558

559 **Table 4** Stern-Volmer quenching constants for interaction of fluorophores and the
560 effective quenching constant in EPS with MB and Pb(II).

	K_a(*10^4L/mol)	K (*10^4L/mol)	K_q (*10^{12}L/mol·S)
Pb(II)	7.97	0.17	0.17
MB	4.94	7.49	7.49

561
562
563

564 Research Highlights

565

566 1. Anaerobic granular sludge was used for treating multi-components wastewater.

567 2. Biosorption capacity was suppressed by the presence of metal ions and dye.

568 3. Interaction between EPS and contaminants were studied by fluorescence
569 spectrum.

570 4. Response surface methodology improved multi-component biosorption process.

571

572